VIII ECCOMAS Thematic Conference on Smart Structures and Materials
SMART 2017
A. Güemes, A. Benjeddou, J. Rodellar and J. Leng (Eds)

PRESTRESS ACCUMULATION-RELEASE (PAR) FOR DAMPING OF FREE VIBRATIONS IN FRAME STRUCTURES. EXPERIMENTAL STUDY OF A LAB-SCALE DEMONSTRATOR WITH PIEZO-ACTUATED SEMI-ACTIVE NODES.

ARKADIUSZ MRÓZ*†, JAN HOLNICKI-SZULC† AND KRZYSZTOF SEKUŁA*

*Adaptronica Sp. z o. o.
ul. Szpitalna 32, 05-092 Łomianki, Poland
e-mail: amroz@adaptronica.pl, ksekula@adaptronica.pl, web page: http://www.adaptronica.pl

† Institute of Fundamental Technological Research, Polish Academy of Sciences (IPPT)
Department of Intelligent Technologies
ul. Pawińskiego 5B, 02-106 Warsaw, Poland
e-mail: holnicki@ippt.pan.pl - Web page: http://www.ippt.pan.pl

Key words: Adaptive Structures, On-Off Control, Variable Stiffness Joint

Abstract. This paper presents results of experimental tests of a demonstrator structure equipped with variable stiffness nodes for suppression of free vibrations. So called Prestress Accumulation-Release (PAR) strategy for on-off control of these nodes is utilized. The obtained system is semi-active. The core of the controllable nodes are linear piezo-actuators.

1 INTRODUCTION

So called Prestress Accumulation-Release strategy, which allows for conversion of portions of strain energy of a vibrating structure into kinetic energy of local, well damped, higher frequency vibrations, has been discussed in preceding publications. In particular in [1] and [2] this approach has been numerically applied to layered and frame structures respectively. The effectiveness of this semi-active technique appears to be extremely high, typically suppressing over 90 % of the fundamental mode of vibrations after only few free oscillation periods. Therefore an attempt has been made to build a demonstrator and verify the theoretical effectiveness in a series of lab tests. First a concept of an active structural joint has been elaborated and presented in [3]. A chosen literature overview is also given in [3] pointing at other concepts for semi-active suppression of structural vibrations. In addition the attention is drawn to [4], in which a linear active element is presented capable of controlling the axial force transferred via a truss member. The goal of present work, which is a continuation of [3], is to present in detail the manufactured active joint as well as to present results of tests, in which two active joints were built into a

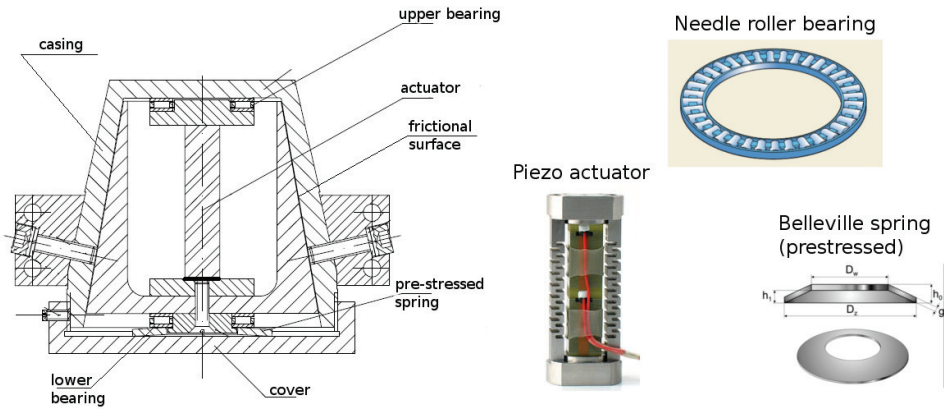

Figure 1: Adaptive node cross-section with its internal components.

demonstrator frame structure and utilized in accordance with PAR strategy to mitigate free vibrations.

2 PAR NODE CONCEPT AND REALIZATION

The active device suitable for demonstration of the PAR strategy should allow to transfer possibly big moment in its "stiff" or "frame" state and reduce its stiffness as close to zero as possible in its "truss" state. Furthermore the active device should sustain its maximum stiffness in passive operation which makes it fail safe.
Major features of the adaptive node are shown on the cross-section depicted in Figure 1. The core of the adaptive node is Cedrat prestressed piezo-actuator PPA 40L which allows for high force generation (order of 3000 N at small weight and dimensions, and at very small stroke (order of 40 μm). The inner conical surface is in contact with the outer conical surface, thus producing the frictional resistance to applied moment depending on the contact normal force between the adjacent surfaces. The conical fit assembly is described in detail in [5]. The normal force in turn depends on the net force produced by the actuator and the prestressed disc spring. Thus the maximum moment transferred by the connection may take any value between the rated maximum, corresponding to 150 V applied to piezo stacks and the minimum corresponding to no voltage applied. In practice the minimum value is never zero because of imperfectly matched spring force, imprecision in actuator nest manufacturing and bearing imperfections. More details about the PAR node concept can be found in [3].

3 STATIC MODEL

A simplified mathematical model of the adaptive node has been elaborated allowing for analysis of static forces acting within a node in both passive and active operation. The main goal for this model was adequate choice of the node body stiffness, pre-stressed spring stiffness and the estimation of the spring initial displacement. Moreover the model allows for verification of the effective actuator force and the maximum moment transferred without slip.
A simple physical model, which has been elaborated is based on the adaptive node layout shown in Figure 1 and comprises all meaningful elements in terms of static response, i.e.:

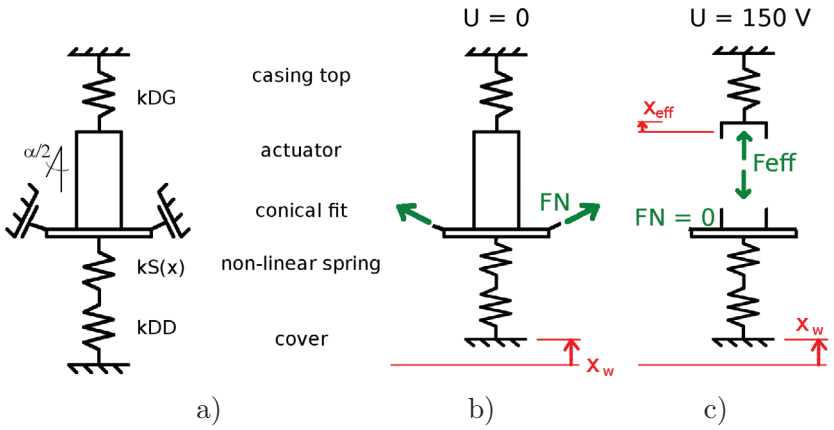

Figure 2: Physical model of the adaptive node: a) main components, b) passive state, c) active state.

- two springs in series, one modelling the cover deflection (kDD) and one modelling the non-linear Belleville spring ($kS(x)$),
- a force representing interaction between the inner part of the node and the casing,
- an actuator force as a function of applied voltage,
- a linear spring connected in parallel with the actuator and modelling stiffness of the upper part of casing (kDG),
- all springs are connected on one side with rigid base, modelling the stiff part of the casing.

Assumed physical model of the adaptive node is shown in Figure 2a).

3.1 Passive operation

In passive operation no voltage is applied to the piezoelectric stacks. It was assumed that the compressive force generated with the pre-stressed spring is entirely transferred to the casing through the conical surfaces and hence the force in the actuator is practically zero (cf. Fig. 2 b)). This is possible provided precise machining of the actuator nest. Pre-stressing of the spring is obtained with applying to it displacement x_w by means of a fine threaded cover. The force F_N normal to the conical fit is given with equation:

$$F_N = \frac{F_A}{\sin(\alpha/2) + \mu\cos(\alpha/2)}, \tag{1}$$

where μ is the friction coefficient and α is the cone angle. F_A is the axial compressive force in the node obtained by equating spring forces in serial connection:

$$F_A = \frac{kS\,kDD}{kS + kDD} \cdot x_w, \tag{2}$$

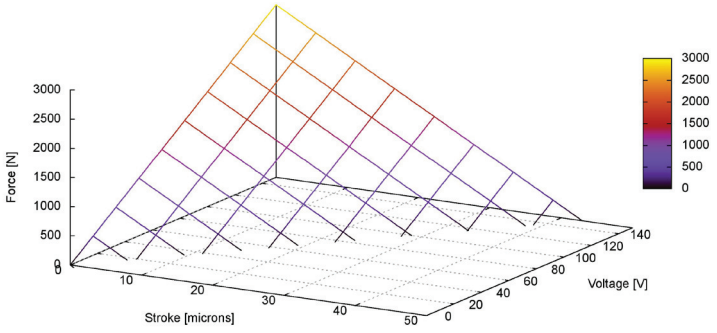

Figure 3: Characteristic of Cedrat Technologies actuator type PPA40L.

where kS is the Belleville spring stiffness linearised in vicinity of the pre-stress deflection. In fact, the Belleville springs have strong non-linear characteristic, therefore the axial compression force is obtained iteratively from the equation:

$$Fs(x1) = kDD \cdot (x_w - x1), \tag{3}$$

where $x1$ is the deflection of the disc spring. The maximum moment M_f which may be transferred via the connection is obtained from the slip condition for frictional conical surfaces with middle diameter dm:

$$|M_f| - \mu\, 0,5\, dm\, F_N \leq 0. \tag{4}$$

3.2 Active operation

In active state voltage is applied to the piezoelectric stacks and the resulting effective force in the actuator is equal to:

$$F_{act} = -\frac{u}{u_{max}} \cdot FB + \frac{V}{V_{max}} \cdot FB. \tag{5}$$

Characteristic calculated according to equation (5) for a chosen actuator is shown in Fig. 3.

It can be seen that the maximum blocking force FB is actually obtained at maximum applied voltage V_{max} only if the actuator is fully blocked, i.e. stroke u equals zero. Otherwise the actuator force is decreased by amount proportional to the stroke. We assume that the adaptive node design is optimal if the actuator at its nominal voltage is able to cancel out the axial force generated by the pre-stressed spring thus reducing the friction force between the conical surfaces to zero. Such situation is shown in Fig. 2 c). The design objective is therefore to maximize the moment bearing capability of the adaptive node in passive mode on one hand while providing enough actuation force to reduce, preferably to zero, the transferred moment in active mode – on the other hand. The effective force (and stroke) in the actuator depends on the stiffness of the casing top. The effective force and stroke corresponding to the steel casing top $\phi 55\, mm$ and thickness between $2\, mm$ and $5\, mm$ is shown in Figure 4. For example at casing thickness equal to 5mm the maximum effective force equals $3643\, N$ which is 88% of the nominal blocking force.

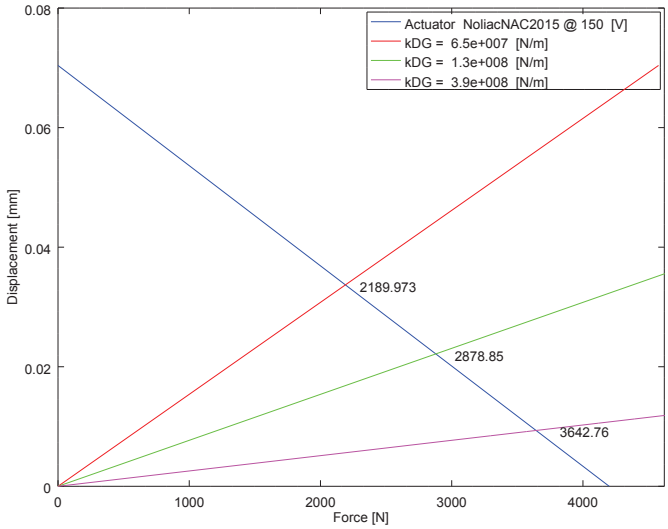

Figure 4: Values of maximum effective force in a chosen actuator at various stiffness of the casing top.

The pre-stressed disc spring dimensions and its initial displacement should allow sufficient pressure in the frictional surfaces, while not exceeding the actuator effective force. Various configurations have been analysed, finally converging to commercially available disc spring of the characteristic shown in Figure 5. Shown operating point corresponds to $0,8\,mm$ initial displacement and the maximum moment in static operation equal to ca $47\,Nm$.

4 DEMONSTRATOR STAND

A simple demonstrator has been built to verify the effectiveness of adaptive nodes in mitigation of free vibrations. The demonstrator structure comprises a cantilever steel frame equipped with two adaptive nodes as shown in Fig. 6. The main elements of the assembled experimental stand are (numbers in accordance with Fig. 7):

1. frame structure,
2. semi-active PAR nodes equipped with Cedrat Technologies PPA40L actuators,
3. two channel, controllable voltage amplifier for piezo stacks actuation Cedrat LA75B-2,
4. control and data acquisition measurement card National Instruments USB-6211,
5. laser vibrometer OFV-505 (5a) with controller (5b),
6. work station with LabView software for data acquisition and control.

During the tests the vibration velocity of the top end of the structure is recorded with laser vibrometer. The same control signal is applied to the piezoelectric stacks of both actuators in accordance with the PAR control strategy. In addition longitudinal vibrations were measured with two accelerometers placed in vicinity of adaptive nodes. Three types of tests have been carried out:

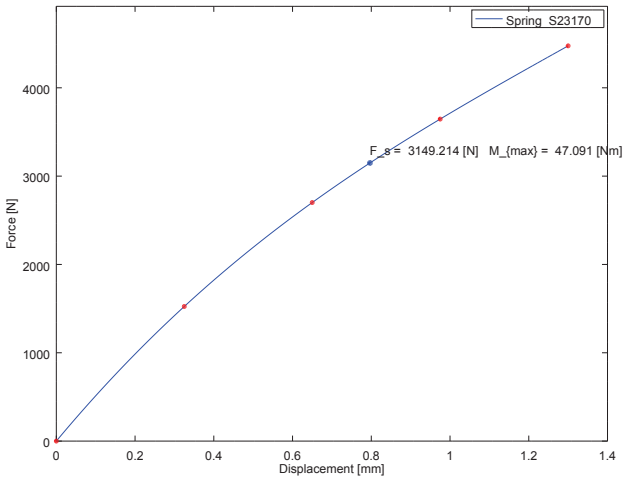

Figure 5: Characteristic of the used spring with the operating point at $0,8\,mm$.

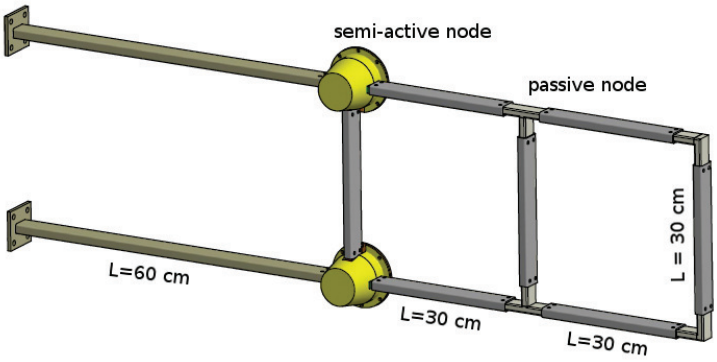

Figure 6: Cantilever beam with two adaptive nodes.

- free vibrations with adaptive nodes in passive state (max. stiffness),
- free vibrations with adaptive nodes in active state (min. stiffness),
- free vibrations with adaptive nodes controlled in accordance with PAR strategy.

The goal of first two tests was to compare the frequency response of acceleration in order to estimate shift in the eigen frequency between the passive and active state of operation. A considerable shift in in-plane bending eigen frequency would be a good indicator that the change of operation mode of adaptive nodes indeed contributes to the overall stiffness of the structure and thus some mitigation effect might be expected.

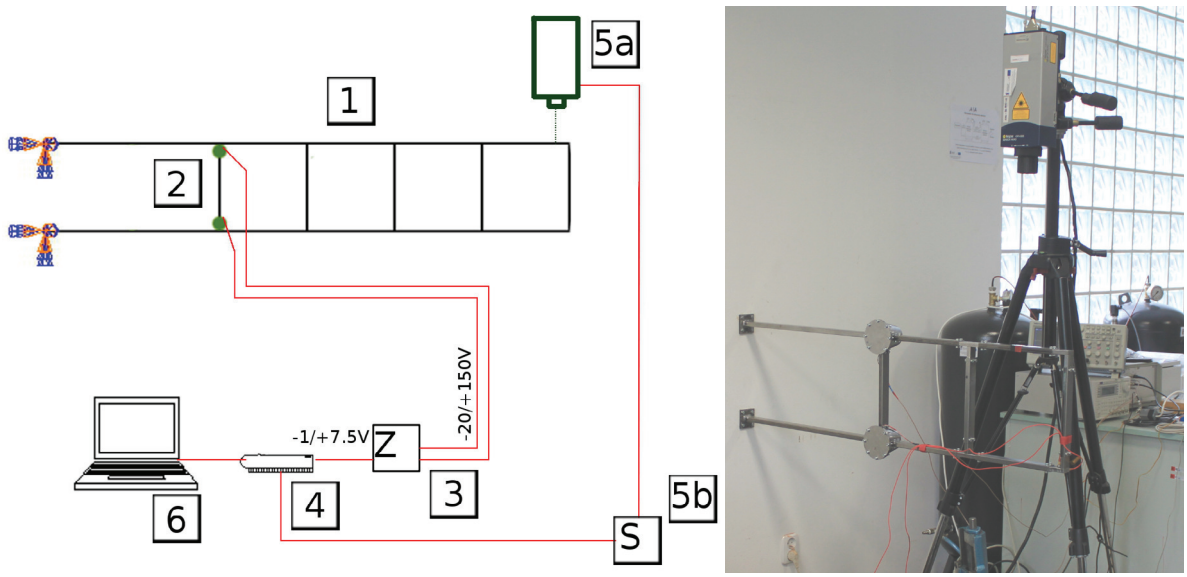

a) b)

Figure 7: Experimental stand: a) Schematic representation, b) General view.

5 RESULTS OF EXPERIMENTS

5.1 Node characteristic

Both adaptive nodes have been tested for their individual characteristic. For this purpose the outer conical surface have been fixed, while a known, increasing force have been applied on a known geometric eccentricity to the inner conical surface until the slip. The maximum moment in the connection corresponding to the beginning of slip is calculated for various actuator control voltage, giving the individual characteristic shown in Fig. 8. The actually obtained maximum moments between 55 and 59 Nm are underestimated by the static model, which may be attributed to the difficulty in accurate regulation of the initial displacement of disc springs. Satisfactory compliance is obtained if the value of $0,95\,mm$ is used instead of $0,80\,mm$. Further it can be observed that the actual moment transferred is not zero at maximum actuation voltage. Some friction still exists on the frictional surfaces even at maximum applied actuator effective force probably because insufficient precision in machining of the actuator nest. Nevertheless obtained variation in moment bearing capability between ca. 6 and 56 Nm provides fairly large range for modification of local stiffness if the adaptive node is used as a structural element. Relative to its mass and dimensions the adaptive node prototype seems to be an efficient variable stiffness device, compared for example to magneto-rheologic fluid based devices.

5.2 Eigen frequency shift

In the first two series of tests of the demonstrator structure adaptive nodes worked either in passive (frame) mode and active (truss) mode. In both cases an initial displacement has been applied to the cantilever end initiating the free in-plane vibrations. The first out-of-plane eigen mode have been sufficiently separated, so that the vertical initial displacement initiates

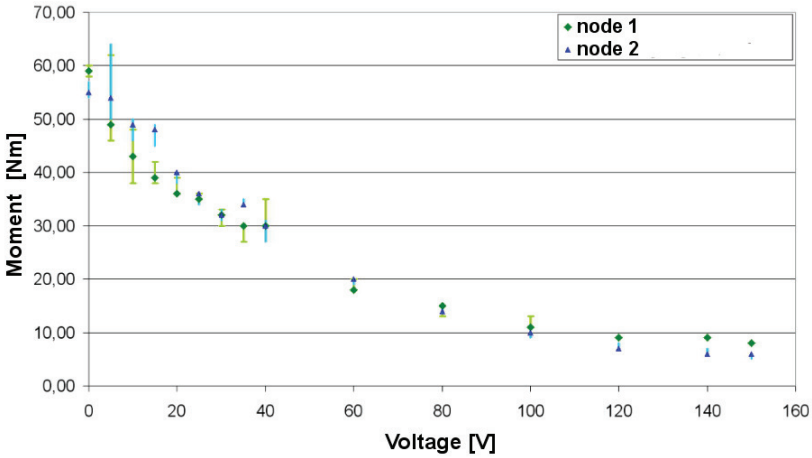

Figure 8: Moment characteristic of two adaptive nodes.

mostly the in-plane vibrations. The frequency response based on the cantilever tip acceleration (differentiated vibrometer velocity signal) is compared in Fig. 9. It can be seen that the first in-plane eigen mode in the truss operation is shifted left by 26 % and accompanied by generally higher damping while the second in-plane eigen mode stays practically unchanged (cf. Table 1). The higher damping is due to some friction corresponding to the remaining moment in truss mode operation.

Table 1: Eigen frequencies of the demonstrator structure in frame (ω_f) and truss(ω_t) modes.

Mode shape No	Description	$\omega_f\,[Hz]$	$\omega_t\,[Hz]$	Difference [%]
1	1^{st} in-plane bending	14.1	10.4	26.2
2	2^{nd} in-plane bending	38.5	38.1	0.9

5.3 Vibration mitigation

In the third series of tests adaptive nodes have been controlled in accordance with the PAR strategy. Upon detection of maximum cantilever deflection adaptive nodes have been switched to the active state for a short period of time, after which the passive state has been restored. As result the structural stiffness have been reduced locally for a very short period of time, sufficient to introduce high frequency, well damped longitudinal vibrations. Each time such operation is repeated, a part of the mechanical energy is transferred to the higher frequency vibrations and effectively damped with material damping.
As can be seen in the typical time series shown in Fig. 10 the vibration amplitude of the fundamental mode is almost completely damped out. The remaining vibrations correspond to the second in-plane bending eigen mode and could possibly by reduced if more adaptive nodes were used and placed in positions optimal for the second eigen mode mitigation. The reference tests

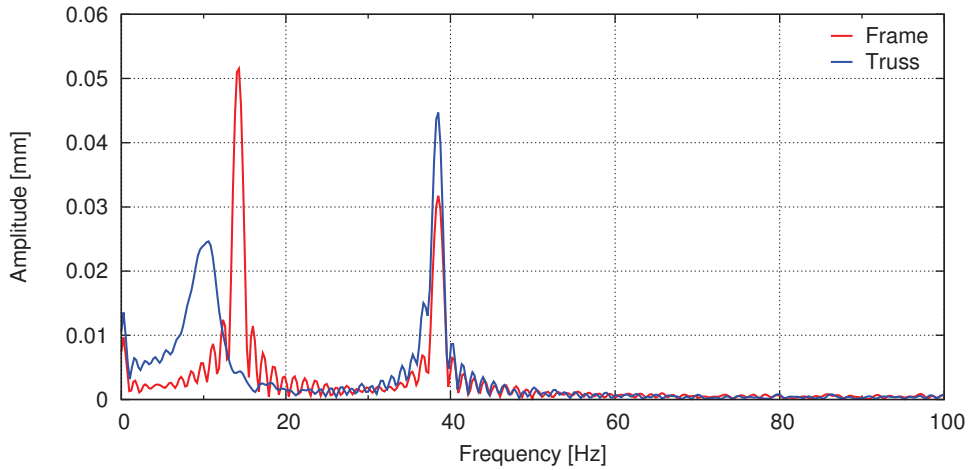

Figure 9: Difference in free vibration frequency response between structure with adaptive nodes in passive operation (frame mode) and in active operation (truss mode).

correspond to the passive operation where no control signal is applied and the adaptive nodes work at their maximum stiffness.

The control procedure has been activated upon first detection of threshold displacement ($+0,1\,mm$ in this case) and deactivated half a second later. During this time period the on-off PAR control algorithm produced the control signal as shown in Fig. 11. In fact, no further advantage is taken of a longer time duration of the control activation. This is due to the fact that after initial half a second the remaining vibration amplitudes do not generate moments in adaptive nodes which exceed the minimum moment transferred through the connection. As result there is no difference between the active and passive mode and no further mitigation occurs, except the "normal" damping in the passive operation.

For each recorded displacement time series the successive amplitude values were compared with the initial amplitude value (equal ca. $1,0\,mm$). In particular, the ratio of the amplitude after 3^{rd}, 6^{th} and 10^{th} oscillation periods to the initial amplitude are listed in Table 2 both for the reference case and for six controlled tests. Over 97 % of the amplitude have been mitigated after 10 oscillation periods with adaptive nodes as compared to ca. 35 % for the reference case.

As shown in Fig. 11 the time duration t_i of a single rectangle impulse signal is very short, equal

Table 2: Comparison of vertical displacement amplitudes after 3, 6 and 10 oscillation periods.

No of oscillation cycles	Relative amplitude %						
	w/o control	with control, Test No					
	REF	1	2	3	4	5	6
3	88,6	84,1	33,8	49,9	33,5	78,6	34,5
6	76,0	7,4	8,2	5,5	8,9	15,0	11,7
10	64,4	2,1	3,8	1,3	2,3	2,1	2,9

to $5\,ms$ in this case. Different values of t_i were tested to investigate its influence on the overall

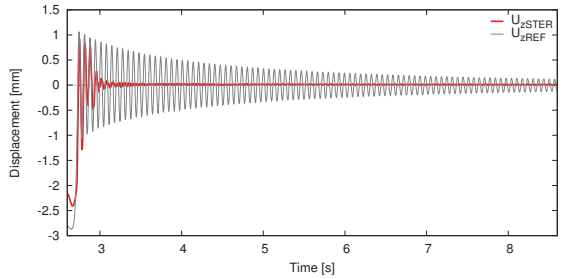

a)

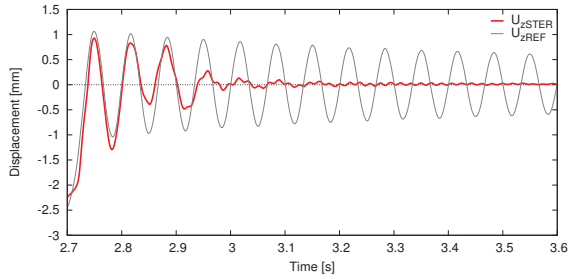

b)

Figure 10: Typical vertical displacements of the cantilever tip: a) full time history, b) zoomed time window.

response. In general time t_i should be long enough to fully switch the adaptive node to the truss mode, taking into account the dynamics of the actuator and accompanying electronics, but on the other hand it should be short so as to not weaken the structure for excessive amount of time. Furthermore too long duration of a single truss mode results in general in frictional dissipation instead of releasing of prestress resulting in longitudinal vibrations which is the main feature of the PAR strategy. In an extreme case the overall damping of the structure permanently operating in truss mode should be much smaller than overall damping of the structure subjected to the actuation in accordance with PAR strategy. This is confirmed with the tests performed for varying duration of a single truss mode t_i between $2\,ms$ and $30\,ms$, as shown in Table 3. The optimum time duration used in subsequent tests was $5\,ms$.

In the optimal situation the truss mode is actually initiated in the adaptive node at the time

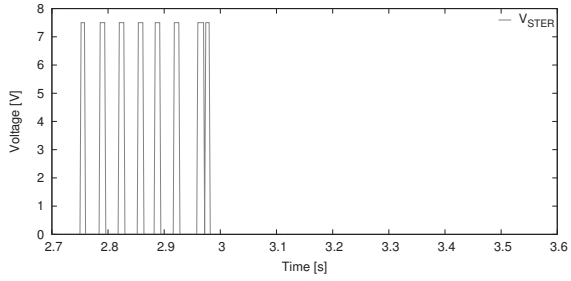

Figure 11: Typical control signal applied to the piezostack controller.

Table 3: Comparison of vertical displacement amplitudes after 5 oscillation periods relative to the initial amplitude, for different t_i.

	Truss mode duration t_i [ms]								
	2	3	4	5	6	8	10	20	30
Relative amplitude %	89	88	40	17	22	18	17	36	78

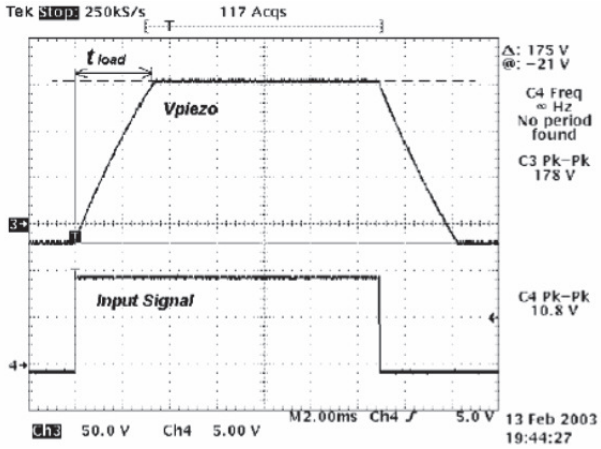

Figure 12: Step response of Cedrat LA-75B voltage amplifier according to the manufacturer.

instant of zero velocity, which corresponds to maximum deflection and maximum strain in the adjacent members. In practice two factors were identified which introduce the offset to the optimum time:

1. the voltage amplifier which drive the piezo-actuators introduces the time constant so that rectangular signal set is actually applied as trapezoid signal to the piezo stacks (cf. Figs. 12 and 13),

2. in order to filter out false triggers on the velocity signal, a short moving averaging has been done before detection of the zero velocity.

Due to above reasons some effort is needed before a good truss mode initiation time is obtained based on the filtered velocity signal. In this proof-of-concept work simple trial-and-error method was sufficient to tune the system performance and the further work requires better tools to properly find the switching time and also a better, impulse voltage amplifier could be used for this on-off control algorithm.

6 CONCLUSIONS AND POSSIBLE APPLICATIONS

- A piezo-based active structural joint with variable moment bearing capability has been designed, built and used as active element in a demonstrator frame structure as a core of semi-active free vibration suppression system.

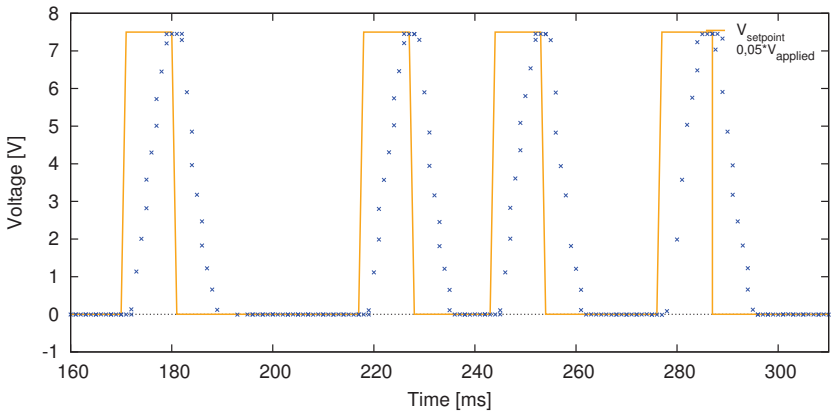

Figure 13: Set control signal versus voltage actually applied to piezo stacks.

- It was demonstrated in a series of experimental tests that utilizing PAR control strategy in such a system allows for very efficient mitigation of fundamental mode of vibrations, typically suppressing 95 % of the displacement amplitude after 10 oscillation cycles.
- The system may be redesigned, given a specific application, in particular it may be downscaled to mitigate microvibrations of a light-weight structures. Among possible applications are mitigation of vibrations of satellites, stabilisation of sensitive equipment and other situations where excessive vibration affects the performance of equipment or generates undesired noise.

ACKNOWLEDGEMENT

Financial support of the National Science Centre, Poland, granted through the project AdDAMP (DEC-2014/15/B/ST8/04363) is gratefully acknowledged.

REFERENCES

[1] A. Mroz, A. Orlowska, and J. Holnicki-Szulc. Semi-active damping of vibrations. prestress accumulation-release strategy development. *Shock and Vibration*, 17(2):123–136, 2010.

[2] A. Mróz, J. Holnicki-Szulc, and J. Biczyk. Prestress accumulation-release for damping of impact borne vibrations. numerical analysis of simple frame fructures. In *Proc. of the 6th World Conference on Structural Control and Monitoring*. Barcelona, Spain, 15-17 July 2014.

[3] A. Mróz and J. Holnicki-Szulc. Mechanical energy management for semi-active damping of impact borne vibrations. In *Proc. of the 7th ECCOMAS Thematic Conference on Smart Structures and Materials*. Ponta Delgada, Azores, Portugal, 3-6 June 2015.

[4] Junjiro Onoda, Takao Endot, Hidehiko Tamaoki, and Naoyuki Watanabe. Vibration suppression by variable-stiffness members. *AIAA journal*, 29(6):977–983, 1991.

[5] Adrian Creitaru and Niculae Grigore. Tribological considerations regarding the functional domain determination of the conical fit assembly. *Machine Design*, 3(3):199–204, 2011.